6-2009

Universal Scaling Behavior in Startup Shear of Entangled Linear Polymer Melts

Pouyan E. Boukany
University of Akron Main Campus

Shi-Qing Wang
University of Akron Main Campus, swang@uakron.edu

Xiaorong Wang

Universal scaling behavior in startup shear of entangled linear polymer melts

Pouyan E. Boukany and Shi-Qing Wang[a)]

Department of Polymer Science, University of Akron, Akron, Ohio 44325-3909

Xiaorong Wang

Bridgestone Americas Center for Research and Technology, Akron, Ohio 44317

(Received 30 June 2008; final revision received 12 January 2009)

Synopsis

We have studied stress overshoot behavior in startup shear of four monodisperse polymer melts with a range of chain entanglement from $Z=24$ to 160 entanglement points per chain. In the elastic deformation regime defined by $\dot{\gamma}\tau_R > 1$, where τ_R is the Rouse relaxation time, (i) the peak shear stress σ_{max} scales with the time t_{max} at the peak to $-1/2$ power, in contrast to an exponent of $-1/4$ in the viscoelastic regime (for $\dot{\gamma}\tau_R < 1$), (ii) σ_{max} changes linearly with the elapsed strain at the stress peak γ_{max}, which scales with the applied shear rate as $\dot{\gamma}^{1/3}$, (iii) a supermaster curve collapses time-dependent shear stress growth curves up to the stress maximum at all shear rates for all the four styrene-butadiene rubber samples.
 [DOI: 10.1122/1.3086872]

I. INTRODUCTION

Polymeric liquids display interesting flow behavior such as wall slip, shear thinning, die swell, melt fracture associated with either roughness on, or distortion of extrudate surface. One of the most widely known rheological responses in entangled polymers is emergence of stress overshoot during sudden (startup) shear at a sufficiently high rate, corresponding to the Weissenberg number $\mathrm{Wi}=\dot{\gamma}\tau > 1$ [Huppler *et al.* (1967); Lee *et al.* (1970); Graessley (1974); Ferry (1980); Menezes and Graessley (1982)]. This transient feature has been widely reported in polymeric liquids from semidilute solutions [Osaki *et al.* (2000a, 2000b, 2000c)], unentangled melts [Moore *et al.* (1999); Santangelo and Roland (2001)] to well entangled polystyrene (PS) solutions [Osaki *et al.* (1975); Crawley and Graessley (1977); Attane *et al.* (1985); Demarquette and Dealy (1992); Pattamaprom and Larson (2001)], polybutadiene (PBD) [Menezes and Graessley (1982); Tapadia and Wang (2004); Robertson *et al.* (2004); Ravindranath and Wang (2008)] and polyisoprene (PIP) solutions [Pearson *et al.* (1989)], and melts [Vinogradov and Belkin (1965); Schweizer (2002); Schweizer *et al.* (2004); Collis *et al.* (2005); Auhl *et al.* (2008)],

Recent particle-tracking velocimetric (PTV) studies [Wang (2007)] in well entangled

[a)]Author to whom correspondence should be addressed; electronic mail: swang@uakron.edu

TABLE I. Molecular characteristics of SBR melts.

Sample	M_w (g/mol)	M_w/M_n	Styrene (%)	Butadiene (%)	Vinyl (1,2-BD) (%)
SBR100K	94 800	1.05	10	90	78.8
SBR170K	174 000	1.07	20	80	65.2
SBR250K	250 000	1.04	20	80	65.0
SBR500K	497 000	1.19	20	80	52.1

solutions [Tapadia and Wang (2006); Boukany and Wang (2007); Ravindranath *et al.* (2008)], DNA [Boukany *et al.* (2008); Boukany and Wang (2009a)], and wormlike micellar solutions [Boukany and Wang (2008)] have shown that entangled network suffered inhomogeneous shear after stress maximum $\sigma_{\max}$, during startup shear. Similar inhomogeneous deformation was found in uniaxial extension of entangled polymer melts after maximum of engineering stress σ_{engr} [Wang *et al.* (2007b); Wang and Wang (2008)]. These observations revealed that the entanglement network could yield to fast large deformation [Wang *et al.* (2007a)]. With $\text{Wi} \gg 1$, a significant amount of elastic deformation takes place until the point of yielding, when the resistant (elastic retractive) force measured in terms of either shear stress or tensile engineering stress can no longer grow with further external deformation. Beyond the yield point, molecular sliding occurs to cause rearrangement of the state of chain entanglement, allowing the stress to decline in time [Wang and Wang (2009)]. The PTV experiments show that the yielding becomes observable in the form of transient elastic recoil and shear banding beyond the stress overshoot in highly entangled solutions [Ravindranath *et al.* (2008)].

Regarding the stress peak in startup shear as the yield point, we are interested in determining salient features associated with the stress overshoot as a function of the level of chain entanglement in melts. In the present study, we have carried out systematic rheometric measurements to explore the transient rheological responses to fast startup shear of monodisperse styrene-butadiene rubber (SBR) melts with the number of entanglements per chain ranging from $Z=24$ to 160. This is made possible by employing a sliding plate rheometer. PTV measurements confirm that homogenous deformation prevails up to the stress overshoot, as expected based on previous studies of solutions [Tapadia and Wang (2006); Boukany and Wang (2007, 2008); Ravindranath *et al.* (2008); Boukany *et al.* (2008)]. Further flow birefringence observations indicate that the sample is intact during shear toward the stress overshoot. All four monodisperse SBR melts of different levels of chain entanglement show the same yielding characteristics in the elastic deformation regime and can be described by the same simple scaling laws that were previously observed in entangled polymer solutions [Ravindranath and Wang (2008)].

II. EXPERIMENTAL

A. Materials and linear viscoelastic properties

A series of monodisperse styrene-butadiene rubber (SBR) with a range of molecular weight M_w from 100 to 500 K was synthesized by anionic polymerization in Bridgestone-America. The microstructural details of these SBR melts are presented in Table I. Small amplitude oscillatory shear [(SAOS) strain amplitude $\gamma=5\%$] was carried out to determine linear viscoelastic properties of these melts with an advanced rheometric expansion system (ARES) using a parallel plate geometry with a diameter of 15 mm and a gap of

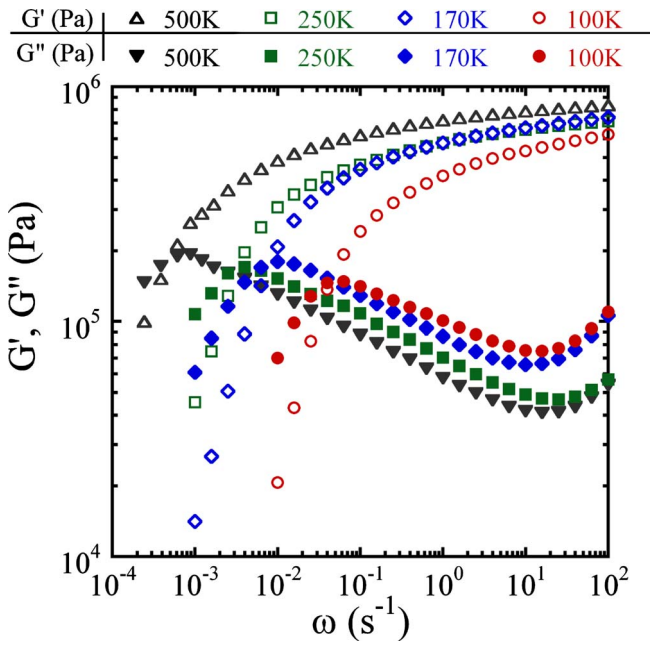

FIG. 1. Small amplitude oscillatory shear (SAOS) measurements of storage and loss moduli G' and G'' for SBR melts of different molecular weights ($T=23$ °C; PP-15 mm).

about 1 mm at room temperature ($T=23$ °C). Figure 1 shows storage and loss moduli G' and G'' as a function of frequency ω for all four SBR melts. The molecular characteristics of these samples based on linear viscoelastic measurements are listed in Table II. The plateau modulus G_N^0 was estimated from the value of G' at the frequency where G'' shows a minimum from which the entanglement molecular weight M_e is estimated according to $G_N^0=\rho RT/M_e$, with the melt mass density $\rho=0.93$ g/cm^3, and R being the gas constant. SBR 100 K has slightly higher styrene content, thus lower G_N^0. The terminal relaxation time τ is estimated as the inverse of the crossover frequency ω_c where $G'=G''$. The Rouse relaxation time τ_R of these entangled melts can be estimated from the terminal relaxation time τ as $\tau_R=\tau/(M_w/M_e)$. One can also estimate τ_R in an empirical way that satisfies its quadratic scaling with M_w [Osaki *et al.* (2001)]. The value estimated from the melt viscosity η is slightly lower and also involves the assumption of 3.4 molecular weight scaling of η. See the footnote following Osaki *et al.* (2001).

TABLE II. Material characteristics based on linear viscoelastic measurements at $T=23$ °C.

Sample	M_e (g/mol)	G_N^0 (MPa)	$Z=M_w/M_e$	τ (s)	$\tau_R=\tau(M_w/M_e)$	G_{coh} [a] (MPa)
SBR100K	4 000	0.55	24	25	1.1	0.27
SBR170K	3 300	0.67	53	120	2.3	0.33
SBR250K	3 300	0.68	76	310	4.1	0.30
SBR500K	3 100	0.72	160	2100	13	0.34

[a]Calculated according to $G_{\text{coh}}=\sigma_{\max}/\gamma_{\max}$ in startup shear mode when $\dot{\gamma}>\tau_R^{-1}$.

B. Experimental apparatus and measurements

In this work, a custom-built sliding plate rheometer (SPR) was employed to produce startup simple shear. The schematic depiction of our SPR involving a stationary bottom plate and movable top plate has been provided previously [Boukany and Wang (2007)]. In a typical startup shear experiment, the step motor is programmed to move suddenly at a prescribed velocity until reaching a given displacement. All of our measurements took place at room temperature ($T \sim 23$ °C).

Bubble-free films of SBR melts were prepared by solution casting and CRAVER press to produce uniform thickness. A sample with a sufficient length L, width W, and thickness H on the orders of $L \sim 3$ cm, $W \sim 1$ cm, and $H \sim 0.05-0.08$ cm, was used. A thin layer (around 10 μm in thickness) of a commercial cyanoacrylate-based super glue (e.g., Instant Krazy® glue) was used to adhere the sample to the two plates so that wall slip is prevented during shear.

In addition, direct visual inspection was carried out during and after measurements. When interfacial failure was observed, the measurement would be discarded. Moreover, flow birefringence observations were conducted from the transparent sliding plates to confirm integrity of the sample during rheological measurements. Armed with such evidence, it is permissible to compute the shear stress σ from the force read with a load cell and the actual area of the sample in each loading that is determined by knowing the gap distance and weight of the sample, along with its mass density ρ.

III. RESULTS AND DISCUSSIONS

A. Stress overshoot in startup shear for SBR-100 K (Z=24)

Typically, when imposed shear rate $\dot{\gamma}$ is greater than $1/\tau$, stress overshoot emerges during startup shear. The peak position can be specified by its coordinates in terms of the stress maximum $\sigma_{\max}$, the corresponding time $t_{\max}$, or the elapsed strain at the peak $\gamma_{\max} = \dot{\gamma} t_{\max}$. Figure 2(a) shows the time-dependent stress as a function of time at various discretely imposed shear rates ($\dot{\gamma}\tau > 1.0$) for the SBR100K melt. Two scaling regimes appear in terms of how $\sigma_{\max}$ varies with $t_{\max}$,

$$\sigma_{\max}(t, \dot{\gamma}) \sim (t_{\max})^{-1/2}, \quad \dot{\gamma} > \tau_R^{-1}, \tag{1}$$

which has been labeled the elastic deformation regime [Wang *et al.* (2007a)] and

$$\sigma_{\max}(t, \dot{\gamma}) \sim (t_{\max})^{-1/4}, \quad \tau^{-1} < \dot{\gamma} < \tau_R^{-1}, \tag{2}$$

which is the viscoelastic regime.

This overshoot character can also be represented on linear scales to show how the stress changes with the elapsed strain $\gamma = \dot{\gamma} t$, as shown in Fig. 2(b). Remarkably, the peak stress $\sigma_{\max}$ is seen to be linear in $\gamma_{\max}$ for the startup shear involving rates in the elastic deformation regime. The slope represented by the dashed line actually reveals a specific modulus G_{coh},

$$\sigma_{\max} = G_{\text{coh}} \times \gamma_{\max}, \tag{3}$$

where the subscript "coh" stands for the material stiffness at the point of yield or cohesive failure. Emergence of such a linear relationship implies that the elastic deformation might be understood to be entropic in origin and to involve linear deformation of a Gaussian chain network. This modulus G_{coh} also tabulated in Table II for all four melts is lower than the initial (intrinsic) modulus G_{int} by a factor of 2.3. It is also interesting to note that $G_{\text{int}} \sim 0.6$ MPa is very close to the plateau modulus G_N^0 determined from Fig. 1. Thus, we

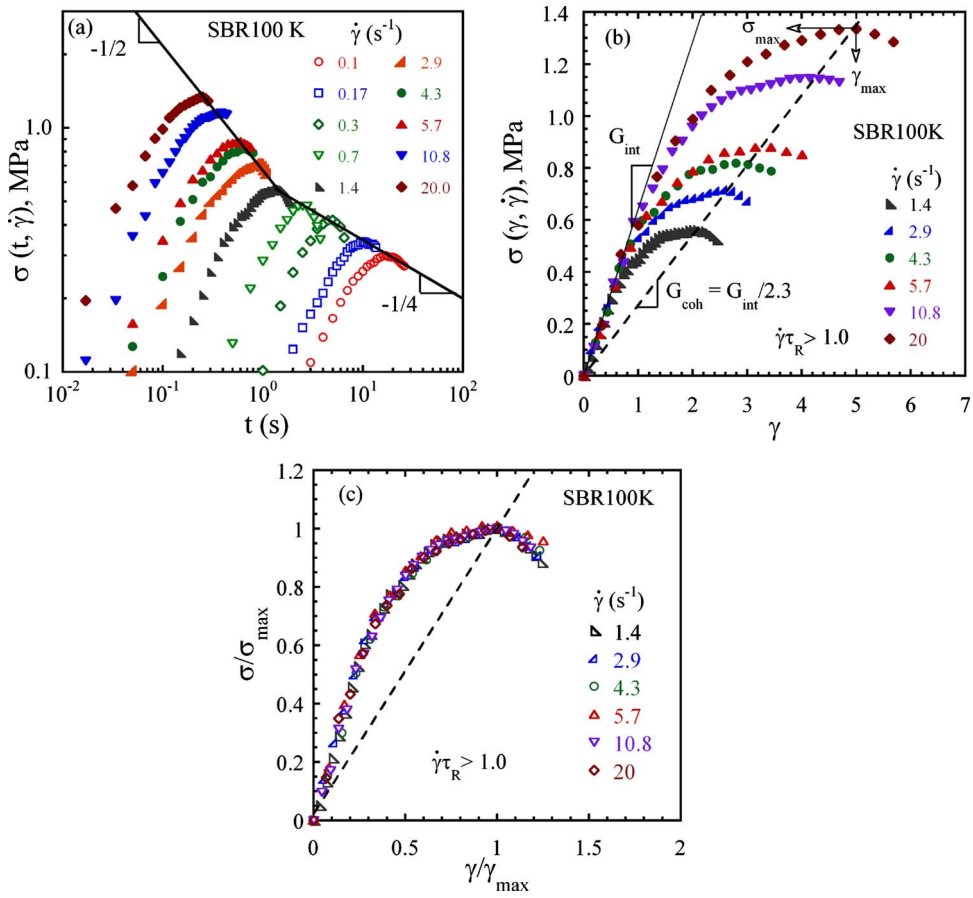

FIG. 2. (a) The growth of shear stress as a function of time at various imposed shear rates for SBR-100 K. (b) σ as a function of the elapsed strain γ in the elastic deformation ($\dot{\gamma}\tau_R > 1$). (c) Master curve of σ growth against γ in the elastic regime obtained by normalizing the curves in (b) with peak values of σ_{max} and γ_{max}, respectively.

conclude that $G_{coh} = G_N^0/2.3$. The subsequent data show that this relationship holds approximately true for all the four SBR melts.

It is instructive to normalize the shear stress σ and strain γ with their respective peak values. Figure 2(c) shows that all data obtained at different rates collapse onto a single master curve. Existence of such a master curve in the elastic deformation regime suggests that the physical origin of stress maximum is the same and the system approaches the yielding point in the same manner at all rates in this elastic deformation regime.

B. Universal scaling laws in all entangled SBR melts (from $Z=24$ to $Z=160$)

It is important to determine whether the characteristics associated with the stress overshoot revealed in Sec. III A remain universal and can be depicted in the same way for melts of different levels of chain entanglement. By increasing the SBR molecular weight, we are able to increase the number of chain entanglements per chain from 24 to 160. Performing startup shear experiments in our sliding plate rheometer, we observe the same features as seen for SBR100K. For example, Figs. 3(a)–3(c) indicate for the other three melts the same relationship of shear stress versus shear strain as shown in Fig. 2(b)

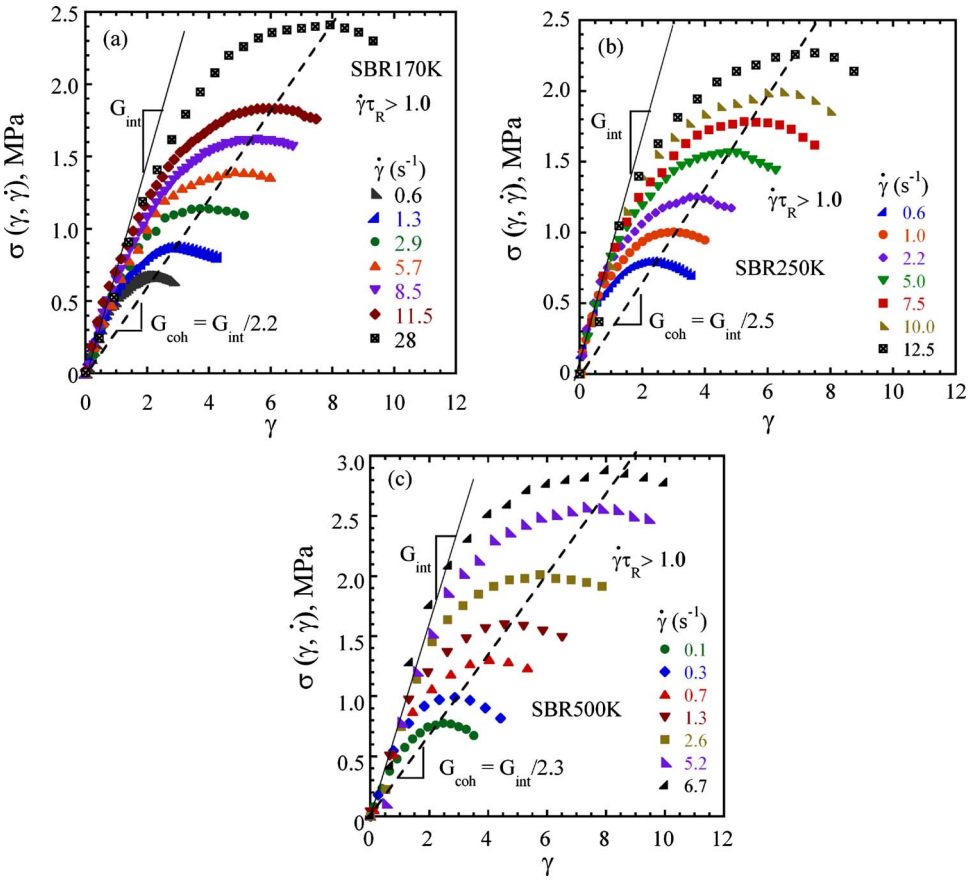

FIG. 3. The growth of shear stress as a function of γ at various imposed shear rates in the elastic deformation ($\dot{\gamma}\tau_R > 1$) for (a) SBR 170 K, (b) SBR 250 K, and (c) SBR 500 K.

under the condition of $\dot{\gamma}\tau_R > 1$, where the "cohesive modulus" $G_{\rm coh}$, evaluated from these plots as the slope of the dashed line and listed in Table II, is universally a factor of approximately 2.3 below the plateau modulus G_N^0 and the intrinsic modulus $G_{\rm int}$ defined in Figs. 2(b) and 3(a)–3(c). Actually, all these curves collapse onto a single super master curve in the normalized coordinates as shown in Fig. 4.

Another way to represent the scaling results in the elastic deformation regime is to make a master curve as shown in Fig. 5(a) where the linearity between $\sigma_{\rm max}$ and $\gamma_{\rm max}$ is demonstrated to involve the same modulus independent of the value of Z, i.e., the slope of $0.43 \sim 1/2.3$ being the same for all four samples. Similarly, extracting from the raw data such as those presented in Fig. 2(a), we obtain in Fig. 5(b) a master curve that depicts the characteristics of the shear stress overshoot, i.e., scaling behavior of the peak stress $\sigma_{\rm max}$ versus the elapsed time $t_{\rm max}$ at the stress maximum, for different applied rates, spanning both the elastic deformation and viscoelastic regimes. Not only do the data collapse together but they also reveal a rather clear separation of dynamic regimes at the Rouse relaxation time τ_R. In particular, Eq. (3) can be rewritten as

$$\sigma_{\rm max} \simeq G_N^0 (\tau_R / t_{\rm max})^{1/2}, \quad \dot{\gamma} > \tau_R^{-1}. \tag{4}$$

Since the elastic deformation regime is found to occur for $t_{\rm max} < \tau_R$, the peak stress is always higher than the elastic plateau modulus G_N^0.

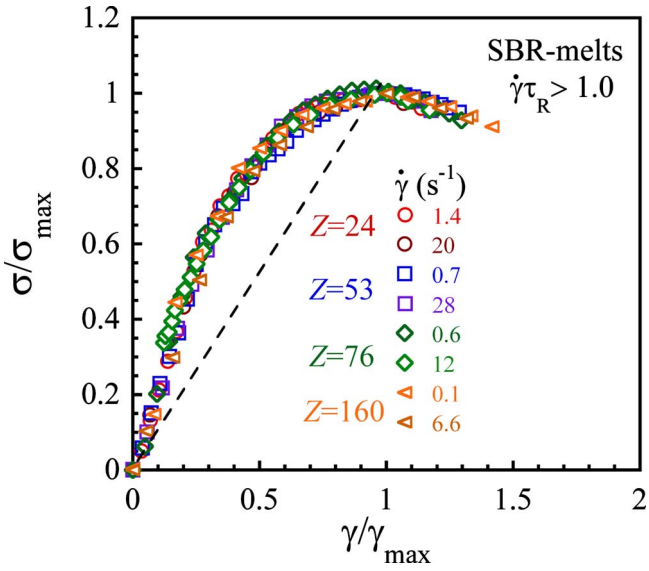

FIG. 4. Supermaster curve of SBR melts in the elastic deformation regime obtained by normalizing the curves in Figs. 2(c) and 3(a)–3(c) with peak values.

Because of the linear relationship of Eq. (3) shown in Fig. 5(a) and the scaling behavior of Fig. 5(b), it is easy to extract an auxiliary scaling law detailing how the position of the yield point, i.e., the shear strain at which the shear stress peaks, γ_{max}, scales with the shear rate. Inserting $\gamma_{max} = \dot{\gamma} t_{max}$ into the combination of Eq. (3) and Eq. (4), we have

$$\gamma_{max} \simeq (\dot{\gamma}\tau_R)^{1/3}, \quad \dot{\gamma} > \tau_R^{-1}. \tag{5}$$

Figure 6 shows the data from all four SBR melts revealing a universal scaling law of Eq. (5) independent of Z, where partial data on polyisoprene melts from Auhl *et al.*

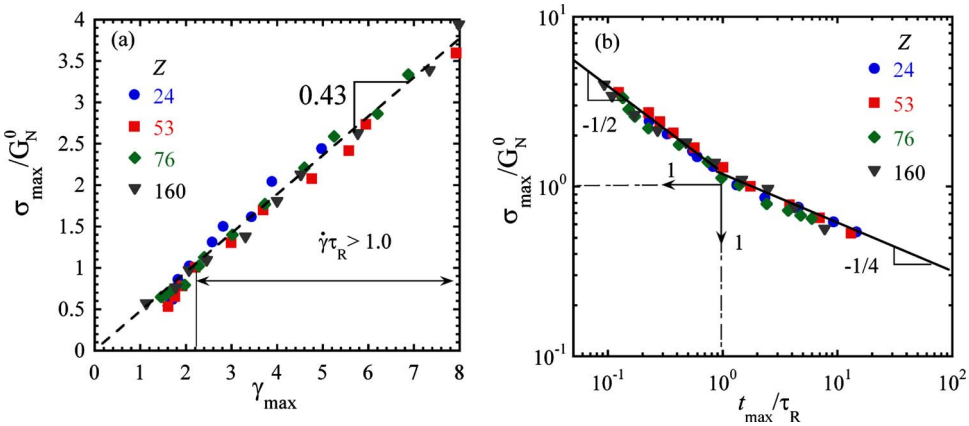

FIG. 5. (a) Master curve for four SBR melts indicating a linear relationship between the σ_{max}/G_N^0 and γ_{max} at the yield point. (b) Master curve for the normalized peak stress σ_{max}/G_N^0 as a function of the normalized time t_{max}/τ_R.

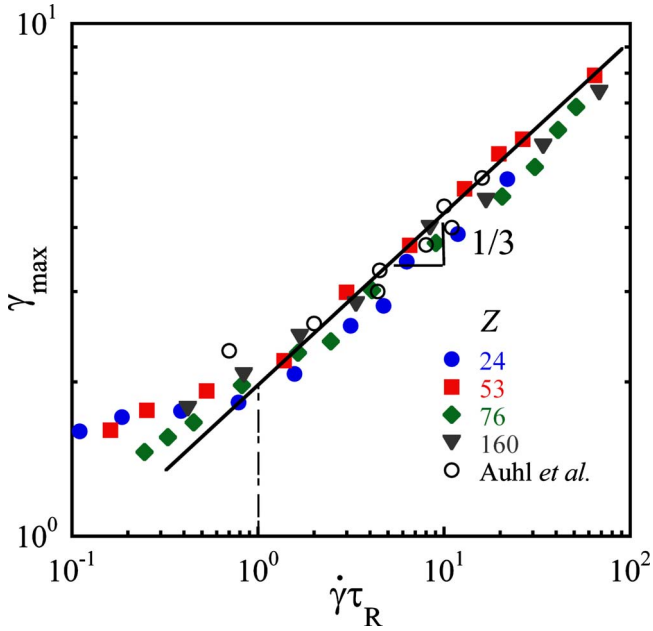

FIG. 6. Master curve for γ_{max} vs $\dot{\gamma}\tau_R$ for all SBR melts, where the open circles are data on polyisoprene (PI) melts from Auhl *et al.* (2008). Because the number of data points from Auhl *et al.* (2008) is low, we take those corresponding to several different molecular weights of PI.

(2008) are incorporated to show agreement and we omitted comparison with the previous data of Schweizer *et al.* (2004) that restricted to just one polystyrene sample and to lower rates.

C. Universality among all entangled liquids

The universal character associated with the shear stress overshoot may actually go beyond these SBR melts. To further explore the universality of the observed scaling laws, we combine the present results with those obtained previously from entangled PBD solutions [Ravindranath and Wang (2008)]. Figures 7(a) and 7(b) show that both entangled solutions and melts are governed by the same scaling laws in both elastic and viscoelastic regimes, where the collapse of data for the different samples onto a single line in Fig. 7(a) is made possible by normalizing the shear stress with the cohesive modulus G_{coh} of each system. A supermaster curve analogous to Fig. 5(a) can also be constructed by adding the data of PBD solutions from Ravindranath and Wang (2008). Figure 8 shows an impressive overlapping of all data onto a universal linear relationship between σ_{max} and γ_{max} valid for the different entangled solutions and melts.

Finally, it is instructive to summarize the yielding response to sudden startup shear of a variety of entangled liquids including wormlike micellar, DNA, synthetic polymer solutions, and melts. The supermaster curve in Fig. 9 asserts that such entangled liquids approach to the yield point in a universal way.

D. PTV measurements and flow birefringence visualization

In this section we carried out PTV and flow birefringence measurement to determine how the deformation takes place and find out whether the sample has suffered any failure

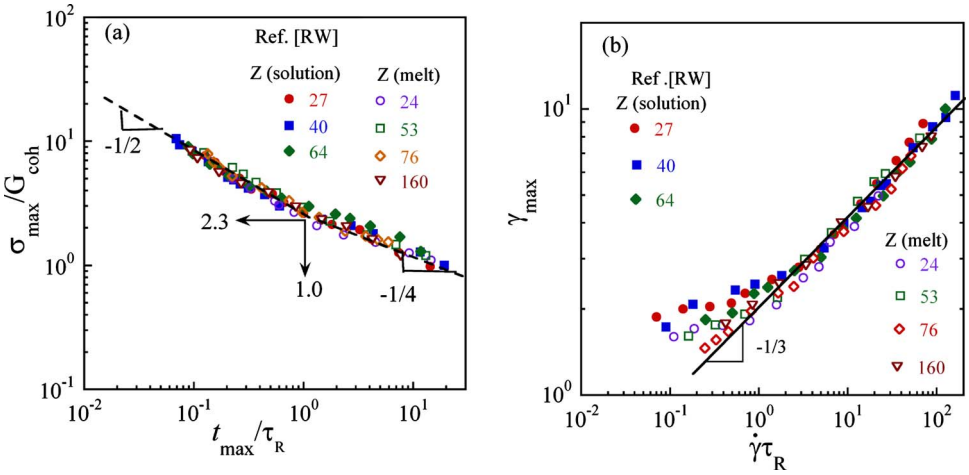

FIG. 7. (a) Supermaster curves for normalized peak stress σ_{max}/G_{coh} as a function of the normalized time t_{max}/τ_R for four melts and solutions with different levels of entanglement obtained from Ravindranath and Wang (2008) [RW], (b) the γ_{max} vs $\dot{\gamma}\tau_R$ for all entangled melts and solutions.

up to the stress maximum. Figures 10(a) and 10(b) show the temporal evolution of stress and velocity profile at $\dot{\gamma}=1.4\ s^{-1}$ for SBR250K. As shown in Fig. 10(b), the deformation is homogeneous until $t=3.3$ s, well after the stress overshoot, although inhomogeneous deformation is clearly visible at $t=4.8$ s.

Since we rely on measurements of the total force to determine the shear stress, it is necessary to ensure that the sample is intact during startup shear to the point of stress overshoot. At a shear rate of $5.7\ s^{-1}$, SBR100K shows its shear stress maximum around

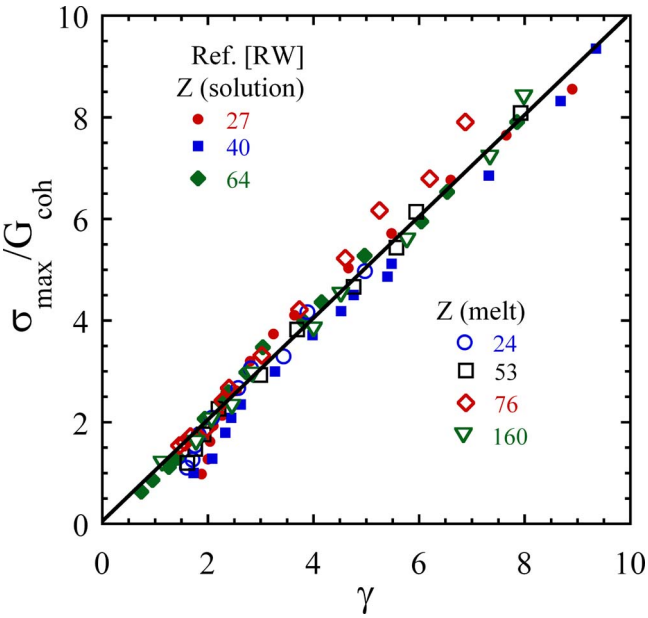

FIG. 8. Supermaster curves for the normalized peak stress σ_{max}/G_{coh} as a function of strain for four melts and solutions with different levels of entanglement [Ravindranath and Wang (2008)].

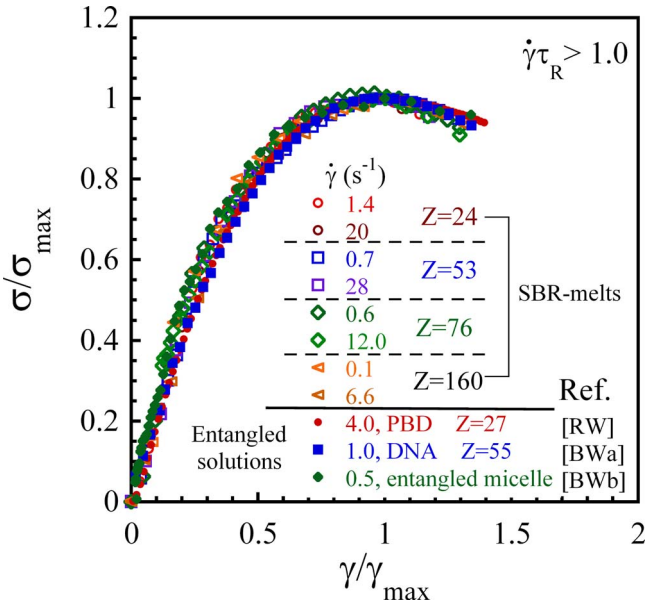

FIG. 9. Supermaster curves for the normalized stress growth σ/σ_{max} as a function of normalized strain γ/γ_{max} for all entangled melts obtained from Fig. 5 entangled PBD from [Ravindranath and Wang (2008)], DNA solutions from Boukany and Wang (2009a) [BWa], and wormlike micellar solution from Boukany and Wang (2008) [BWb].

$\gamma_{max}=3.0$, i.e., at $t_{max}=0.5$ s, according to Fig. 2(b). A flow birefringence setup [Boukany and Wang (2008)], involving placing a halfwave retardation plate between two mutually perpendicular polarizers at 45° to the shearing direction, is used to monitor the sample integrity. Under a white light source, our color charge-coupled device video camera reveals evolution of the optical retardation in Fig. 11 during a startup shear and shows that neither edge fracture nor glue failure takes place during deformation up to the stress maximum.

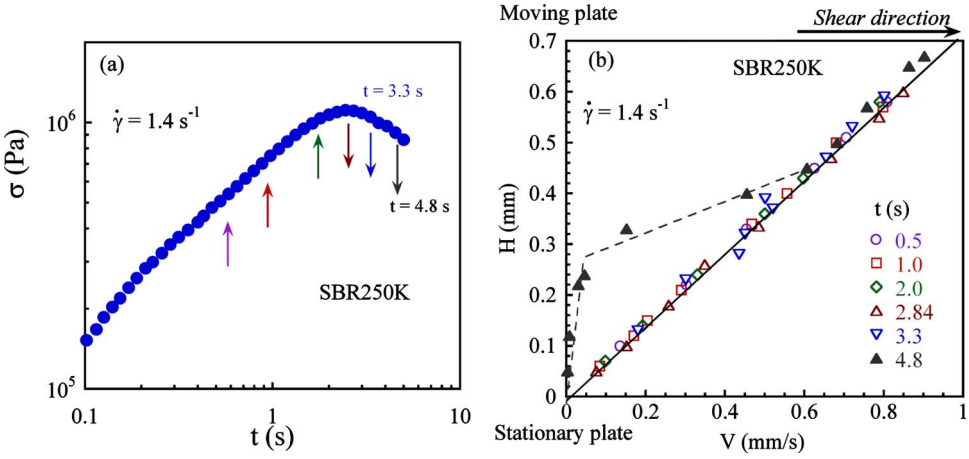

FIG. 10. Time evolutions of (a) shear stress (b) velocity profile for SBR 250 K at $\dot{\gamma}=1.4$ s^{-1}, from $t=0$ to 4.8 s.

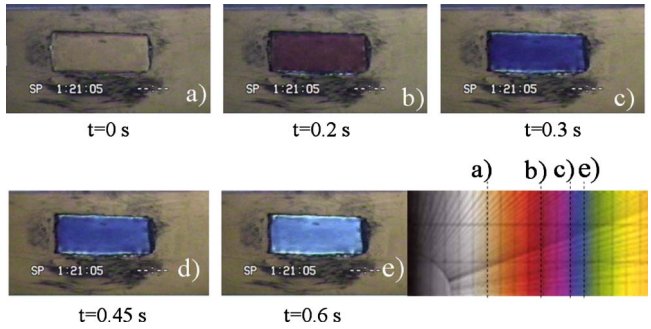

FIG. 11. (Color online) The flow birefringence images at times from $t=0$ to 0.6 s along the velocity gradient direction for SBR 100 K obtained using a full wave retardation plate between two crossed polarizers that are 45° to the shearing direction at $\dot{\gamma}=5.7\ s^{-1}$, where the initial transparency arises from the use of the retardation plate as shown in the Michel-Levy chart with other corresponding retardations also indicated from (a) to (e).

IV. CONCLUSIONS

In this work, we have investigated universal scaling characteristics associated with stress overshoot that occurs during startup shear in SBR melts whose level of chain entanglement ranges from $Z=24$ to 160 entanglements per chain. Specifically, in the elastic deformation regime defined by $\dot{\gamma}\tau_R>1$, we found that at the point of yield, i.e., the moment when the shear stress peaks, the peak shear stress $\sigma_{\max}$ scales linearly with the strain $\gamma_{\max}$ at the peak and both $\sigma_{\max}$ and $\gamma_{\max}$ scales with the applied shear rate with an exponent of 1/3. At lower rates yet still above the terminal flow regime, we see a crossover behavior with $\sigma_{\max}\sim G_N^0(\tau_R/t_{\max})^{1/4}$ and $t_{\max}>\tau_R$ instead of $\sigma_{\max}\sim G_N^0(\tau_R/t_{\max})^{1/2}$ with $t_{\max}<\tau_R$. These scaling laws turn out to be universal, independent of Z, and of whether the sample is a present SBR melt or a previous PBD solution or an entangled DNA solution.

Actually, the whole process of stress growth up to the point of overshoot is universal in the sense that a single supermaster curve can be obtained for the shear stress normalized by its peak value vs the elapsed strain normalized by its value at the stress maximum for all shear rates and all different entangled liquids ranging from PBD, wormlike micellar solutions to DNA solutions, and SBR melts. Existence of such a supermaster curve is likely to encourage us to look for a universal theory that can depict the elastic yielding during startup deformation of well entangled polymeric liquids.

Since the reported universal scaling behavior occurs before any inhomogeneous deformation is to take place subsequently, we expect its theoretical depiction to be more tractable than a full molecular theory for polymer deformation and flow. The latest version of tube model [Graham *et al.* (2003)] seemed to be able to quantitatively describe the observed scaling laws [Auhl *et al.* (2008)]. However, it also appears to be the case [Wang (2008)] that the same theory of Graham *et al.* (2003) cannot depict or anticipate the experimental observations of nonquiescent relaxation in the simpler step strain experiments on both entangled solutions [Ravindranath and Wang (2007)] and melts [Boukany and Wang (2009b)]. It is true that the tube theory does not envision the stress maximum as a yield point, where the entanglement network ceases to undergo further molecular deformation due, according to our understanding [Wang *et al.* (2007b); Wang and Wang (2009)], to a force imbalance between the intermolecular locking force that is causing the

chain deformation and the intramolecular elastic retraction force. Beyond this yield point, the entanglement structure inevitably gets torn apart. This is a concept that is not embedded in the tube theory.

ACKNOWLEDGMENTS

This work is supported, in part, by a small grant for exploratory research (Grant No. DMR 0603951) and a standard grant (Grant No. DMR-0821697) from Polymers program of the National Science Foundation.

References

Attane, P., J. M. Pierrard, and G. J. Turrel, "Steady and transient shear flows of polystyrene solutions. 1. Concentration and molecular weight dependence of non-dimensional viscometric functions," J. Non-Newtonian Fluid Mech. **18**, 295–317 (1985).

Auhl, D., J. Ramirez, A. E. Likhtman, P. Chambon, and C. Fernybough, "Linear and nonlinear shear flow behavior of monodisperse polyisoprene melts with a large range of molecular weights," J. Rheol. **52**, 801–836 (2008).

Boukany, P. E., Y. T. Hu, and S. Q. Wang, "Observations of wall slip and shear banding in an entangled DNA solution," Macromolecules **41**, 2644–2650 (2008).

Boukany, P. E. and S. Q. Wang, "A correlation between velocity profile and molecular weight distribution in sheared entangled polymer solutions," J. Rheol. **51**, 217–233 (2007).

Boukany, P. E. and S. Q. Wang, "Use of particle-tracking velocimetry and flow birefringence to study nonlinear flow behavior of entangled wormlike micellar solution: From wall slip, bulk disentanglement to chain scission," Macromolecules **41**, 1455–1464 (2008).

Boukany, P. E. and S. Q. Wang, "Shear banding or not in entangled solutions depending on the level of entanglement," J. Rheol. **53**, 73–83 (2009a).

Boukany, P. E. and S. Q. Wang, "First evidence of polymer melts undergoing inhomogeneous shear during startup shear and breakup after shear cessation," Macromolecules, submitted (2009b).

Collis, M. W., A. K. Lele, M. R. Mackley, R. S. Graham, D. J. Groves, A. E. Likhtman, T. M. Nicholson, O. G. Harlen, T. C. B. McLeish, L. R. Hutchings, C. M. Fernyhough, and R. N. Young, "Constriction flows of monodisperse linear entangled polymers: Multiscale modeling and flow visualization," J. Rheol. **49**, 501–522 (2005).

Crawley, R. L. and W. W. Graessley, "Geometry effects on stress transient data obtained by cone and plate flow," Trans. Soc. Rheol. **21**, 19–49 (1977).

Demarquette, N. R. I. and J. M. Dealy, "Nonlinear viscoelasticity of concentrated polystyrene solutions-sliding plate rheometer studies," J. Rheol. **36**, 1007–1032 (1992).

Ferry, J. D., *Viscoelastic Properties of Polymers* (Wiley, New York, 1980).

Graessley, W. W., "The entanglement concept in polymer rheology," Adv. Polym. Sci. **16**, 1–179 (1974).

Graham, R. S., A. E. Likhtman, T. C. B. McLeish, and S. T. Milner, "Microscopic theory of linear, entangled polymer chains under rapid deformation including chain stretch and convective constraint release," J. Rheol. **47**, 1171–1200 (2003).

Huppler, J. D., I. F. Macdonal, E. Ashare, T. W. Spriggs, and R. B. Bird, "Rheological properties of three solutions. Part II. Relaxation and growth of shear and normal stresses," Trans. Soc. Rheol. **11**, 181–204 (1967).

Lee, C. L., K. E. Polmanteer, and E. G. King, "Flow behavior of narrow distribution polydimethylsiloxane," J. Polym. Sci., Part A-2 **8**, 1909–1916 (1970).

Menezes, E. V. and W. W. Graessley, "Nonlinear rheological behavior of polymer systems for several shear flow histories," J. Polym. Sci., Polym. Phys. Ed. **20**, 1817–1833 (1982).

Moore, J. D., S. T. Cui, H. D. Cochran, and P. T. Cummings, "Transient rheology of a polyethylene melt under shear," Phys. Rev. E **60**, 6956–6959 (1999).

Osaki, K., M. Fukuda, S. I. Ohta, B. S. Kim, and M. J. Kurata, "Nonlinear viscoelasticity of polystyrene solutions. II. Non-Newtonian viscosity," J. Polym. Sci., Polym. Phys. Ed. **13**, 1577–1589 (1975).

Osaki, K., T. Inoue, and T. Isomura, "Stress overshoot of polymer solutions at high rates of shear," J. Polym. Sci., Part B: Polym. Phys. **38**, 1917–1925 (2000a).

Osaki, K., T. Inoue, and T. Isomura, "Stress overshoot of polymer solutions at high rates of shear; polystyrene with bimodal molecular weight distribution," J. Polym. Sci., Part B: Polym. Phys. **38**, 2043–2050 (2000b).

Osaki, K., T. Inoue, and T. Uematsu, "Stress overshoot of polymer solutions at high rates of shear: Semidilute polystyrene solutions with and without chain entanglement," J. Polym. Sci., Part B: Polym. Phys. **38**, 3271–3276 (2000c).

Osaki, K., T. Inoue, T. Uematsu, and Y. Yamashita, "Evaluation methods of the longest rouse relaxation time of an entangled polymer in a semidilute solution," J. Polym. Sci. Polym. Phys. Ed. **39**, 1704–1712 (2001). Using Eq. 7 from this paper, i.e., $\tau_{R\eta}=(6M_w\eta/\pi^2\rho RT)(M_c/M_w)^{2.4}$, and taking M_c to be twice M_e, where η is the zero-shear viscosity, we estimate $\tau_{R\eta}$ to be ca. 0.78, 1.9, 3.7, and 9.9 s, respectively, for SBR100K, SBR170K, SBR250K, and SBR500K instead of 1.1, 2.3 and 4.1 and 13 s listed in Table II. These two groups of values are quite similar. Since $\tau_{R\eta}$ for SBR500K is not reliable with the crude estimate of η from Fig. 1, we choose to plot the master curves such as Fig. 6 based on τ_R tabulated in Table II.

Pattamaprom, C. and R. G. Larson, "Constraint release effects in monodisperse and bidisperse polystyrenes in fast transient shearing flows," Macromolecules **34**, 5229–5237 (2001).

Pearson, D. S., A. D. Kiss, L. J. Fetters, and M. Doi, "Flow-induced birefringence of concentrated polyisoprene solutions," J. Rheol. **33**, 517–535 (1989).

Ravindranath, S. and S. Q. Wang, "What are the origins of stress relaxation behaviors in step shear of entangled polymer solutions?" Macromolecules **40**, 8031–8039 (2007).

Ravindranath, S. and S. Q. Wang, "Universal scaling characteristics of stress overshoot in startup shear of entangled polymer solutions," J. Rheol. **52**, 681–695 (2008).

Ravindranath, S., S. Q. Wang, M. Olechnowicz, and R. P. Quirk, "Banding in simple steady shear of entangled polymer solutions," Macromolecules **41**, 2663–2670 (2008).

Robertson, C. G., S. Warren, D. J. Plazek, and C. M. Roland, "Re-entanglement kinetics in sheared polybutadiene solutions," Macromolecules **37**, 10018–10022 (2004).

Santangelo, P. G. and C. M. Roland, "Interrupted shear flow of unentangled polystyrene melts," J. Rheol. **45**, 583–594 (2001).

Schweizer, T., "Measurement of the first and second normal stress differences in a polystyrene melt with a cone and partitioned plate tool," Rheol. Acta **41**, 337–344 (2002).

Schweizer, T., J. van Meerveld, and H. C. Öttinger, "Nonlinear shear rheology of polystyrene melt with narrow molecular weight distribution—Experiment and theory," J. Rheol. **48**, 1345–1363 (2004).

Tapadia, P. and S. Q. Wang, "Nonlinear flow behavior of entangled polymer solutions: Yieldlike entanglement-disentanglement transition," Macromolecules **37**, 9083–9095 (2004).

Tapadia, P. and S. Q. Wang, "Direct visualization of continuous simple shear in non-Newtonian polymeric fluids," Phys. Rev. Lett. **96**, 016001 (2006).

Vinogradov, G. V. and I. M. Belkin, "Elastic, strength and viscous properties of polymer (polyethylene and polystyrene) melts," J. Polym. Sci., Part A: Gen. Pap. **3**, 917–932 (1965).

Wang, S. Q., "A coherent description of nonlinear flow behavior of entangled polymers as related to processing and numerical simulations," Macromol. Mater. Eng. **292**, 15–22 (2007).

Wang, S. Q., "The tip of iceberg in nonlinear polymer rheology: Entangled liquids are 'solids'," J. Polym. Sci., Polym. Phys. Ed. **46**, 2660–2665 (2008).

Wang, S. Q., S. Ravindranath, Y. Wang, and P. Boukany, "New theoretical considerations in polymer rheology: Elastic breakup in chain entanglement network," J. Chem. Phys. **127**, 064903 (2007a).

Wang, Y., P. Boukany, S. Q. Wang, and X. Wang, "Elastic breakup in uniaxial extension of entangled polymer melts," Phys. Rev. Lett. **99**, 237801 (2007b).

Wang, Y. and S. Q. Wang, "From elastic deformation to terminal flow of a monodisperse entangled melt in uniaxial extension," J. Rheol. **52**, 1275–1290 (2008).

Wang, Y. and S. Q. Wang, "New theoretical considerations in polymer rheology: 2.Yielding during startup flow of entangled polymeric liquids," Macromolecules, submitted (2009).